J Appl Physiol 125: 1339–1348, 2018.
First published August 16, 2018; doi:10.1152/japplphysiol.00620.2018.

RESEARCH ARTICLE

Provocative decompression causes diffuse vascular injury in mice mediated by microparticles containing interleukin-1β

Stephen R. Thom, Veena M. Bhopale, Kevin Yu, and Ming Yang

Department of Emergency Medicine, University of Maryland School of Medicine, Baltimore, Maryland

Submitted 9 July 2018; accepted in final form 10 August 2018

Thom SR, Bhopale VM, Yu K, Yang M. Provocative decompression causes diffuse vascular injury in mice mediated by microparticles containing interleukin-1β. *J Appl Physiol* 125: 1339–1348, 2018. First published August 16, 2018; doi:10.1152/japplphysiol.00620.2018.—Inflammatory mediators are known to be elevated in association with decompression from elevated ambient pressure, but their role in tissue damage or overt decompression sickness is unclear. Circulating microparticles (MPs) are also known to increase, and because interleukin (IL)-1β is packaged within these particles, we hypothesized that IL-1β was responsible for tissue injuries. Here, we demonstrate that elevations of circulating MPs containing up to ninefold higher concentrations of IL-1β occur while mice are exposed to high air pressure (790 kPa), whereas smaller particles carrying proteins specific to exosomes are not elevated. MPs number and intra-particle IL-1β concentration increase further over 13 h post decompression. MPs also exhibit intra-particle elevations of tumor necrosis factor-α, caspase-1, inhibitor of κB kinase-β, and inhibitor of κB kinase-γ, and elevated IL-6 is adsorbed to the surface of MPs. Contrary to lymphocytes, neutrophil nucleotide-binding oligomerization domain-like receptor, pyrin domain containing 3 (NLRP3) inflammasome oligomerization and cell activation parameters occur during high pressure exposure, and additional evidence for activation is manifested post decompression. Diffuse vascular damage, although not apparent immediately post decompression, was present 2 h later and remained elevated for at least 13 h. Prophylactic administration of an IL-1β receptor inhibitor or neutralizing antibody to IL-1β inhibited MPs elevations, increases of all MPs-associated pro-inflammatory agents, and vascular damage. We conclude that an auto-activation process triggered by high pressure stimulates MPs production and concurrent inflammasome activation, and IL-1β is a proximal factor responsible for further cytokine production and decompression-associated vascular injuries.

NEW & NOTEWORTHY Elevations in circulating microparticles due to decompression have been documented in humans and animals. This report shows that intra-particle interleukin-1β causes vascular damage that can be abrogated by interventions directed against this cytokine.

exosomes; interleukin-6; nuclear factor-κB; nucleotide-binding oligomerization domain-like receptor, pyrin domain containing 3; neutrophil activation; tumor necrosis factor-α

INTRODUCTION

Decompression sickness (DCS) is a risk associated with compressed-gas diving and tunneling, high-altitude aviation, and space exploration. Intravascular gas bubbles, thought to be an inciting factor for DCS, are common and often asymptomatic, so additional pathophysiological factors have been sought to explain development of the syndrome (13, 31, 32). There is now considerable evidence that microparticles (MPs), vesicles with diameters of ~0.1–1.0 μm that bud from the cell membrane surface, are elevated in association with simulated as well as bona fide underwater diving (36–38, 46, 55, 56, 61).

Maneuvers in humans that decrease the incidence of DCS also diminish MPs production (36, 37). Murine studies indicate that MPs play a role in high pressure gas pathophysiology and possibly with gas bubble nucleation (57, 58, 66, 67). MPs initiate a systemic inflammatory process documented on decompression, and injuries identified in decompressed animals can be recapitulated by injecting decompression-induced MPs into naïve mice (57, 58, 66, 67). Neutrophil activation has a role in these events, as fewer MPs are generated in myeloperoxidase (MPO)-knockout mice over ~24 h post decompression, but other factors possibly including platelets are involved (57).

There is a long history of assaying for pro- and anti-inflammatory mediators in humans and laboratory animals subjected to decompression. Following multiday and provocative diving, humans exhibit elevations in interleukin (IL)-8 and heat shock protein (HSP)-72 (16, 28). Elevations found in animal models include IL-1β, IL-6, IL-8, IL-10, IL-13, tumor necrosis factor (TNF)-α, interferon-γ, transforming growth factor-β, prostaglandin E_2, thromboxane B_2, monocyte chemoattractant protein-1, HSP-1, HSP-32, and HSP-60 (2, 6, 8, 15, 21, 29, 30, 40, 47, 62). However, no direct cause-effect relationships for symptoms or pathology among these agents have been shown with decompression. Demonstrating relationships in association with other disorders has also been poor, although cause-effect has been reported with some autoimmune and diabetic complications (1, 11, 25). Direct associations with these agents are thought to be difficult to prove because of concurrent production of pro-and anti-inflammatory agents, overlapping synthetic pathways, and rapid plasma clearance.

We were especially interested in reports pertaining to IL-1β because of its unusual physiology (8, 62, 63). IL-1β is synthesized in response to oxidative stress and exposure to products released by damaged cells and microorganisms, and by cytokines, including IL-1α and IL-1β itself, IL-18, and TNF-α (11). IL-1β plays a central role in many inflammatory responses because of its autocatalytic production and because it can trigger synthesis of alternative cytokines and other inflammatory agents (11). IL-1β is produced within innate immune cells as an inactive 31-kDa precursor. The pro-IL-1β is cleaved by one of several proteases activated via protein complexes, or

Address for reprint requests and other correspondence: S. R. Thom, 655 W. Baltimore St., Bressler Research Building Rm. 4-013, Baltimore, MD 21201 (e-mail: sthom@som.umaryland.edu).

"inflammasomes," formed with cell stimulation (11, 20). IL-1β cannot be liberated directly to the extracellular milieu. It first requires packaging into vesicles for secretion, either MPs or smaller exosomes (~40–120 nm diameter) produced by secretory autophagy (26, 44). This is because IL-1β is synthesized without a leader peptide, so it cannot utilize the conventional secretory pathway (endoplasmic reticulum-Golgi-plasma membrane) (5, 35, 45, 51). Evidence of a primary pathophysiological role for IL-1β in various disorders comes from studies in which its actions are inhibited by specific blockade with neutralizing antibodies and/or an IL-1β receptor inhibitor (11).

Some cytoskeletal and organelle functions in the synthetic pathway that produces MPs overlap with activation of the nucleotide-binding oligomerization domain-like receptor, pyrin domain containing 3 (NLRP3) inflammasome that generates active IL-1β (51, 52, 54). Following some insults, MPs containing high concentrations of IL-1β are produced, and vascular injuries mediated by these MPs have been linked to this cytokine (51, 52, 54). Given the association between MPs and IL-1β synthesis, we hypothesized intra-MPs IL-1β may be the cause for decompression-induced systemic vascular injuries.

MATERIALS AND METHODS

Materials. Chemicals were purchased from Sigma-Aldrich (St. Louis, MO) unless otherwise noted. Compressed gases were purchased from Air Products and Chemicals, Inc. (Allentown, PA) and anakinra from Amgen (Thousand Oaks, CA). Information on antibodies is summarized in Table 1.

Animals. All aspects of this study were reviewed and approved by the Institutional Animal Care and Use Committee, by the Department of the Navy, Bureau of Medicine and Surgery, and with adherence to the National Institutes of Health *Guide for the Care and Use of Laboratory Animals*. C57BL/6J mice *(Mus musculus)* were purchased from Jackson Laboratories (Bar Harbor, ME), housed in the university animal facility, fed Laboratory Rodent Diet 5001 (PMI Nutritional Inc., Brentwood, MO) and water ad libitum.

Mice were left to breathe room air (control) or subjected to 1- or 2-h exposure to 790 kPa air exactly as described in previous publications (57, 67). Some mice were injected intraperitoneally with 100 mg/kg anakinra, a polyclonal anti-mouse IL-1β neutralizing antibody or a nonspecific control antibody at 50 μg/mouse. Immediately on decompression (*time 0*) or at 2 or 13 h after decompression, mice were anesthetized [intraperitoneal administration of ketamine (100 mg/kg) and xylazine (10 mg/kg)] and euthanized for blood and tissue collection as described previously (57, 67).

Standard procedures for extracellular vesicles analysis. Prior to use all reagents and solutions were filtered with 0.1-μm filter (EMD Millipore, Billerica, MA). Plasma was prepared for analysis as previously described (57, 67). Briefly, heparinized blood was immediately fixed with 100 μl/ml Fixation Medium A (Invitrogen Inc., Carlsbad, CA) and centrifuged for 5 min at 1,500 *g*. EDTA was added to the supernatant to achieve 12.5 mM to minimize extracellular vesicles (EVs) aggregation, then it was centrifuged at 15,000 *g* for 30 min to sediment residual platelets and large protein aggregates, and the supernatant was used for EVs analysis. Where discussed, supernatant was then centrifuged at 21,000 *g* for 1 h to sediment some of the MPs population, and then at 100,000 *g* for 2 h.

EVs analysis. Samples for MPs analysis were labeled for 30 min at room temperature in the dark with optimized concentrations of antibodies (Table 1) in 100 μl filtered Annexin V binding buffer (BD PharMingen, San Jose, CA) and analyzed by flow cytometry as described in detail in prior publications (57). Briefly, studies were performed with an eight-color, triple laser MACSQuant Analyzer (Miltenyi Biotec Corp., Auburn, CA) using MACSQuantify software version 2.5 to analyze data. MACSQuant was calibrated every other day with calibration beads (Miltenyi Biotec Corp.). Forward and side scatter were set at logarithmic gain. Photomultiplier tube voltage and triggers were optimized to detect submicron particles. Microbeads of three different diameters, 0.3 μm (Sigma, Inc., St. Louis, MO) and 1.0 μm and 3.0 μm (Spherotech, Inc., Lake Forest, IL), were used for initial settings and before each experiment as an internal control. Annexin V positive particles with diameters between 0.3 and 1 μm were defined as MPs. The concentration of MPs in sample tubes was determined by MACSQuant Analyzer according to exact volume of solution from which MPs were analyzed.

Particles smaller than MPs that included exosomes were analyzed using a tunable resistive pulse sensing (TRPS) device (qNano Gold instrument, Izon Science USA, Ltd., Cambridge, MA) and also by

Table 1. *Suppliers of antibodies for interventions and analytical assays*

Antibody/Agent	Manufacturer, Cat. No.
Interventional antibodies	
Neutralizing anti-mouse IL-1β antibody	BioXcell, Brandord, CT, cat. no. BE-0246
Nonspecific control IgG	BioXcell, cat. no. BE-0089
MPs assay agents:	
Anti-Ly6G eFluor450	eBioscience, San Diego, CA, cat. no. 48–5931–82
Anti-mouse CD31 BV510	Becton Dickinson/PharMingen, BD, San Jose, CA, cat. no. 563089
Annexin V-FITC	BD, cat. no. 556419
Anti-CD41 PerCP Cy5.5	BioLegend, San Diego, CA, cat. no. 133918
Neutrophil activation assay agents:	
Anti-PR3 FITC	Abcam, Cambridge, MA, cat. no. ab-91182
Anti-mouse MPO PE	Hycult Biotech, Plymouth Meeting, PA, cat. no. HM-1051-PE-100
Anti-mouse Ly6G eFluor450	eBioscience, cat. no. 48–5931–82
Anti-mouse CD41 APC	eBioscience, cat. no. 17–0411–82
Anti-mouse CD284 (TLR4) Alexa Fluor488	eBioscience, cat. no. 53–9041–82
NLRP3 confocal imaging agents:	
Anti-ASC A488	Invitrogen, Carlsbad, CA, cat. no. A-11034
Anti-mouse NALP3 A647	Invitrogen, cat. no. A-21247
Western blotting and dot blot agents:	
Anti-actin	Sigma-Aldrich, St. Louis, MO, cat. no. A-2066
Anti-mouse ASC	Sigma-Aldrich, cat. no. SAB-4501315
Anti-caspase-1 (and pro-caspase-1)	Abcam, cat. no. ab-108362
Anti-mouse IL-1β	Abcam, cat. no. ab-9722
Anti-mouse IL-6	Invitrogen, cat. no. 700480
Anti-mouse IKK-β	Abcam, cat. no. ab-124957
Anti-mouse IKK-γ	Abcam, cat. no. ab-178872
Anti-LAMP1	Abcam, cat. no. ab-178872
Anti-mouse NF-κB	Abcam, cat. no. ab-3243
Anti-TNFα	Abcam, cat. no. ab-9739
Anti-mouse TXNIP	Abcam, cat. no. ab-188865

ASC, apoptosis-associated speck-like protein containing a CARD; IKK, inhibitor of κB kinase; IL, interleukin; LAMP-1, lysosome associated membrane protein-1; Ly6G, lymphocyte antigen 6 complex locus G6D; MPO, myeloperoxidase; MPs, microparticles; NALP3, NACHT, LRR, and PYD domains-containing protein 3; NLRP3, nucleotide-binding oligomerization domain-like receptor, pyrin domain containing 3; PR3, proteinase 3; TLR4, Toll-like receptor 4; TNF, tumor necrosis factor; TXNIP, thioredoxin-interacting protein.

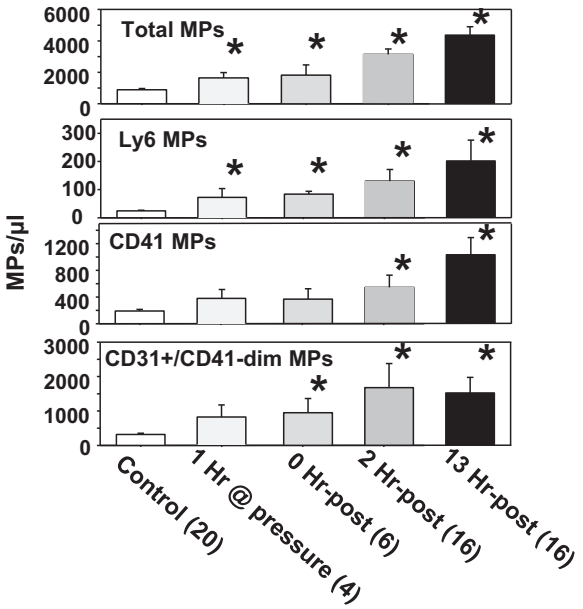

Fig. 1. MPs in mice exposed to 790 kPa air pressure. Blood-borne MPs were quantified in mice euthanized immediately after exposure for 1 or 2 h to 790 kPa air or, in a delayed fashion, at 2 or 13 h after decompression. Flow cytometric measurements were made to quantify the total number of 0.3–1 μm diameter Annexin V-positive particles (*top*), as well as those expressing proteins specific to certain cells: Ly6G (mature neutrophils), CD41 (platelets), and CD31+/CD41-dim (endothelium). Data are mean ± SE, *n* is shown for each sample, *significantly different from control, $P < 0.05$, ANOVA. MPs, microparticles; post, post decompression.

Western blotting. Samples used for TRPS analysis were first passed through a 220-nm filter, and data was obtained using an NP150-rated pore with a fixed stretch of 48 nm, a transmembrane voltage of 0.6 V that gives a baseline current of ~100 nA, and a pressure of 10 millibars. Calibration was done using 100-nm polystyrene beads at a concentration of 1×10^9/ml.

IL-1β measurements and related studies. A mouse-specific ELISA Kit (eBioscience, San Diego, CA) was used to evaluate concentration of IL-1β. Plasma was first combined with equal volume of lysis buffer [20 mM Tris (pH 7.5), 150 mM NaCl, 1% Nonidet P-40, 0.5% sodium deoxycholate, 1 mM EDTA, and 0.1% SDS with protease inhibitors cocktail (Sigma-Aldrich)] and samples analyzed following the manufacturer's instructions. Additional inflammatory mediators were probed by Western blot following published methods (57).

Dot blot analysis of MPs. To evaluate MPs surface versus intravesicle protein cargo, suspensions of 10,000 MPs in 20 μl phosphate buffered saline (PBS) were combined with an equal volume of PBS or PBS containing 2% SDS and 20% glycerol, then placed on nitrocellulose paper and dried. Paper was first treated with blocking buffer (Odyssey, Li-Cor Bioscience, Lincoln, NE) following the manufacturer's protocol and then incubated for 2 h with primary antibody followed by an appropriate secondary antibody for imaging in an Odyssey CLx scanner (Li-Cor Bioscience).

Neutrophil activation analysis by flow cytometry. Whole fixed blood (100 μl) was stained for 30 min at room temperature in the dark with optimized concentrations of antibodies as listed in Table 1. After staining, 2 ml PBS was added to dilute each sample tube before analysis with the cytometer acquisition set to use anti-mouse lymphocyte antigen 6 complex locus G6D protein (Ly6G) as the fluorescence trigger to recognize mouse neutrophils.

NLRP3 oligomerization by Western blot. Following published procedures, isolated neutrophils and lymphocytes were incubated with 0.5 mM dithiobis (succinimidyl propionate) to cross-link sulfhydryl-containing proteins within a proximity of ~12 Å, and lysates were subjected to immunoprecipitation using anti-mouse apoptosis-associated speck-like protein containing a CARD (ASC) and electrophoresed in gradient 4%–15% SDS-PAGE polyacrylamide gels, followed by Western blotting (53).

Confocal microscopy. Images of neutrophils and lymphocytes were acquired using a Nikon inverted stage microscope with antibodies included in Table 1 following procedures as previously described (57).

Vascular permeability assay. Mice were injected via the tail vein with lysine-fixable tetramethylrhodamine-conjugated dextran (2×10^6 Da, Invitrogen) and endothelium-enriched homogenates of brain, omentum, psoas, and quadriceps femoris leg muscle were prepared using colloidal silica following published methods (57). Vascular permeability was quantified as perivascular dextran uptake.

Statistical analysis. Results are expressed as the mean ± SE for three or more independent experiments. Data were compared by *t*-test or, when appropriate, analysis of variance and Newman-Keuls post hoc test using SigmaStat (Jandel Scientific, San Jose, CA). The level of statistical significance was defined as $P < 0.05$.

RESULTS

MPs in mice subjected to pressurization. The impact of exposure to 790 kPa air pressure for 2 h on circulating MPs number is shown in Fig. 1. Statistically significant elevations were found for samples obtained as soon as mice were decompressed (*time 0*) and at 2 and 13 h post decompression. We have not previously examined the MPs count immediately post decompression, and results were surprising, so we also ob-

Table 2. *Neutrophil activation and IL-1β levels*

Group	IL-1β		Neutrophil Activation Relative to Control			
	pg/ml	pg/million MPs	PR3	MPO	TLR4	CD41
Control	13.1 ± 2.2 (24)	9.1 ± 1.1 (17)	1	1	1	1
1 h P	55.7 ± 9.7* (4)	29.9 ± 7.9* (4)	0.86 ± 0.05 (3)	2.33 ± 0.66* (3)	1.00 ± 0.05 (3)	1.25 ± 0.01* (3)
2 h P - 0 h post	137.0 ± 29.6* (8)	81.9 ± 15.5* (8)	1.21 ± 0.08 (7)	1.83 ± 0.38* (7)	0.88 ± 0.22 (7)	1.15 ± 0.06* (7)
2 h P - 2 h post	145.0 ± 28.3* (8)	125.3 ± 21.7* (8)	1.36 ± 0.07* (8)	2.91 ± 0.54* (8)	1.18 ± 0.06* (8)	1.24 ± 0.04* (8)
2 h P - 13 h post	80.5 ± 8.3* (8)	44.1 ± 9.7* (8)	1.48 ± 0.16* (8)	2.44 ± 0.43* (8)	1.05 ± 0.06 (8)	1.21 ± 0.07* (8)
Iso-IgG + 2 h P - 2 h post	121.0 ± 19.4* (4)	78.7 ± 7.8* (4)	1.17 ± 0.05 (4)	1.84 ± 0.33* (4)	0.93 ± 0.05 (4)	1.20 ± 0.04* (4)
IL-1β IgG + 2 h P - 2 h post	27.3 ± 10.2 (4)	41.3 ± 15.6 (4)	1.27 ± 0.25 (4)	2.79 ± 0.53* (4)	1.18 ± 0.09 (4)	1.11 ± 0.05 (4)
IL-1β IgG + 2 h P - 13 h post	23.0 ± 3.8 (4)	10.7 ± 2.0 (4)	1.68 ± 0.33* (4)	1.80 ± 0.28* (4)	1.17 ± 0.09 (4)	0.99 ± 0.02 (4)
Anakinra + 2 h P - 2 h post	14.0 ± 5.4 (4)	40.5 ± 14.7 (4)	1.50 ± 0.18 (4)	2.79 ± 0.53* (4)	1.37 ± 0.06* (4)	1.01 ± 0.04 (4)
Anakinra + 2 h P - 13 h post	19.5 ± 4.4 (4)	20.2 ± 7.7 (4)	1.44 ± 0.28 (4)	1.90 ± 0.28* (4)	1.34 ± 0.16* (4)	1.01 ± 0.03 (4)

Values are mean + SE, *n* = no. of mice (in parentheses). IL, interleukin; Iso-IgG, control IgG; MPO, myeloperoxidase; P, at pressure; post, post decompression; PR3, proteinase 3; TLR4, Toll-like receptor 4. *$P < 0.05$.

tained blood from mice euthanized after just 1 h at 790 kPa pressurization and found elevations of MPs (Fig. 1).

MPs were probed for membrane surface proteins specific to neutrophils (Ly6G) and platelets (CD41), and we also sought evidence for MPs of endothelial origin, as they have been shown to be elevated in relation to a variety of vascular stresses (3, 59). Endothelial MPs exhibit CD31 (platelet-endothelial cell adhesion molecule) but not platelet-specific CD41. Elevations of neutrophil and endothelial MPs were present in samples obtained after 1 h at 790 kPa and at all 3 time points following 2 h at 790 kPa, whereas platelet-derived MPs were elevated at 2 and 13 h post decompression.

Plasma IL-1β and vascular injury assessed as dextran extravasation. Plasma IL-1β concentration was probed by ELISA (first column, Table 2). Statistically significantly elevations were found in samples from mice exposed to elevated pressure. To approach the question of whether IL-1β had a pathological effect, vascular injury was evaluated in mice injected before pressurization with a neutralizing antibody to IL-1β, a control nonspecific IgG antibody, or anakinra. Vascular leak, assessed as rhodamine-dextran uptake, was not statistically significantly different from control in tissues immediately after decompression (Fig. 2*A*), but increases found at 2 and 13 h post decompression were consistent with several published reports (57, 58). Mice injected with neutralizing anti-IL-1β or anakinra did not exhibit vascular leak at 2 h post decompression, in contrast to mice injected with a nonspecific control antibody (Fig. 2*B*). At 13 h post decompression, vascular leakage was seen in omentum of mice treated with antibody to IL-1β but not in mice treated with anakinra (Fig. 2*C*).

Inflammasome formation/activation. We sought evidence for oligomerization of the NLRP3 inflammasome in circulating leukocytes. Cells imaged by confocal microscopy were probed for ASC and cryopyrin or NALP3 (NACHT, LRR, and PYD domains-containing protein 3), which co-localize with inflammasome activation. Co-localization was exceedingly rare in control cells and commonly observed with post-decompression neutrophils. The appearance differed between cells isolated at *time 0* vs. 2 h post decompression (Fig. 3). Rare co-localization was noted in lymphocytes, with no discernible differences between cells from control and decompressed mice.

To confirm NLRP3 oligomerization, proteins in isolated neutrophils and lymphocytes were cross-linked and then lysates prepared for immunoprecipitation using antibody to ASC. Pull-down of NALP3, pro- and mature IL-1β, caspase-1, and an accessory protein, thioredoxin-interacting protein (TXNIP), were markedly greater with neutrophils from decompressed mice versus controls (Fig. 4). The fold-elevations of proteins pulled down in decompressed samples relative to controls run at the same time are shown. Lymphocyte results are not shown,

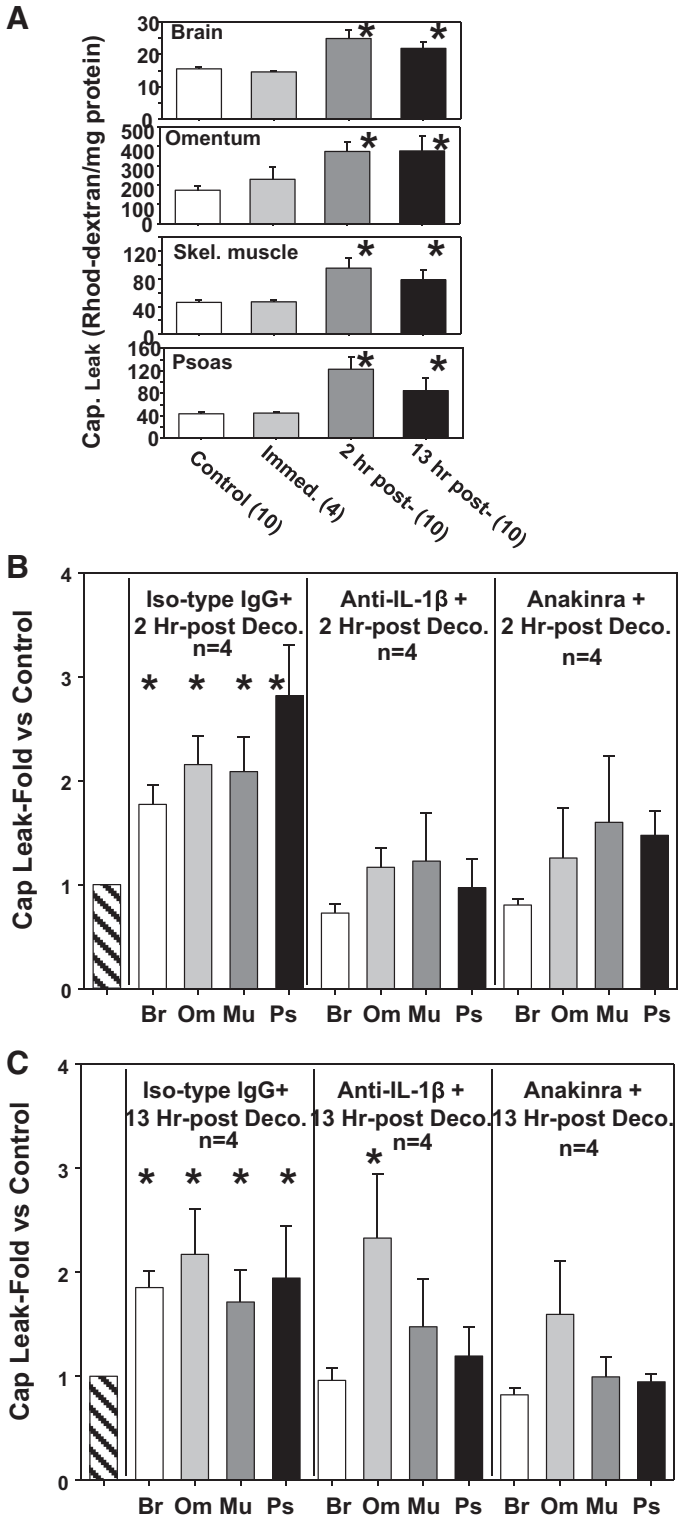

Fig. 2. Vascular leakage of 2×10^6 Da rhodamine-labeled dextran. Mice were euthanized immediately after exposure for 2 h to 790-kPa air or, in a delayed fashion, at 2 or 13 h after decompression. Extravasation of dextran in brain, omentum, leg skeletal muscle, and psoas was evaluated as described in MATERIALS AND METHODS. Data in *A*, *B*, and *C* are mean ± SE, *significantly different from control, $P < 0.05$, ANOVA, sample number indicated as (*n*). *A*: time course. Values reflect rhodamine-dextran fluorescence as arbitrary units/mg protein in tissue homogenates. *B*: protective effect of antibody against IL-1β and anakinra at 2 h post decompression. Mice were injected intraperitoneally with either a nonspecific control IgG, a neutralizing antibody to IL-1β, or anakinra before pressurization and euthanized 2 h post decompression. Data are expressed as relative to rhodamine fluorescence in saline-injected control mice to ease comparison. *C*: protective effect of antibody against IL-1β and anakinra at 13 h post decompression. Mice were injected as outlined in *B* and euthanized at 13 h post decompression. Br, brain; Deco, decompression; IL, interleukin; Iso-type IgG, control IgG; Mu, leg skeletal muscle; Om, omentum; post, post decompression; Ps, psoas.

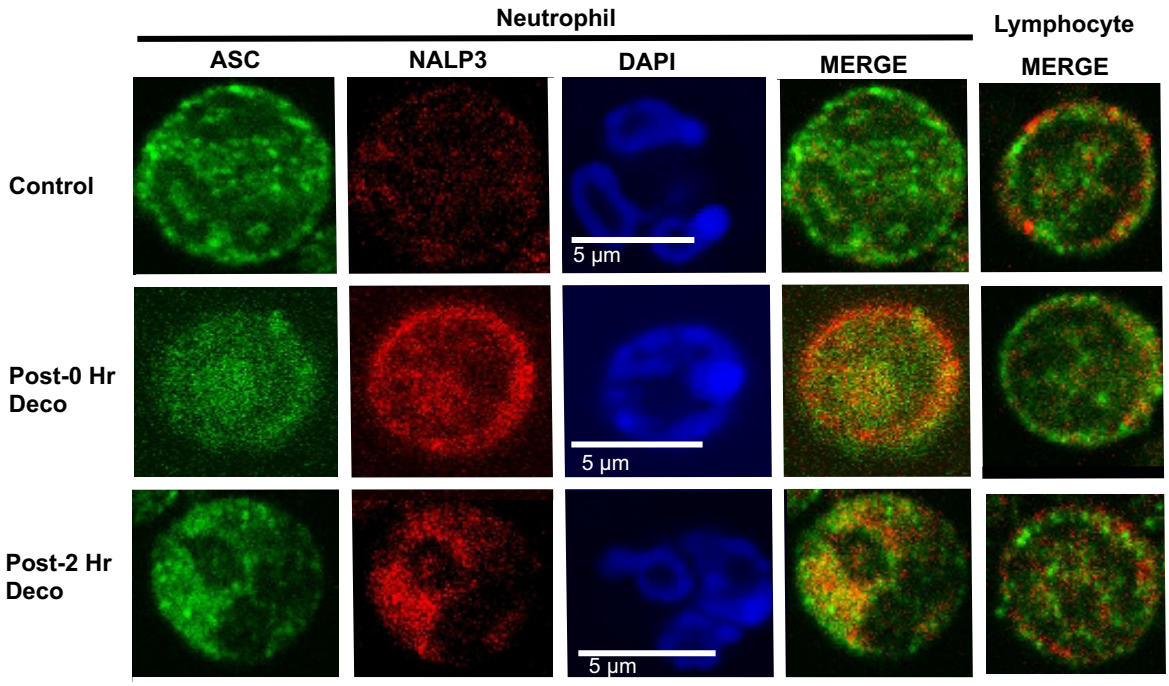

Fig. 3. Confocal micrograph images of isolated mouse neutrophils and lymphocytes. Images were obtained using cells isolated from the blood of control mice and those euthanized either immediately or 2 h after exposure to 790 kPa air pressure for 2 h. Permeabilized cells were stained with antibodies to ASC or NALP3, along with 4′,6-diamidino-2-phenylindole (DAPI) to identify nuclei. Overlap between ASC and NALP3 is shown as yellow in the merged images. Nominal overlap was observed in control neutrophils and lymphocytes from control and decompressed mice (far right set of images). ASC, apoptosis-associated speck-like protein containing a CARD; Deco, decompression; NALP3, NACHT, LRR, and PYD domains-containing protein 3.

as there were no significant differences in band densities between control versus decompressed mice.

Mouse neutrophil activation. Further evidence of neutrophil activation was sought by flow cytometry analysis of surface expressed proteinase 3 (PR3), MPO, and Toll-like receptor 4 (TLR4) on cells identified as neutrophils by surface Ly6G expression. Presence of neutrophil-platelet aggregates were evaluated by probing for platelet-specific CD41 on the neutrophil surface. Elevations of activation parameters on cells from mice exposed to pressure/decompression were found at all time points, as shown in Table 2. Interestingly, administration of anti-IL-1β antibody or anakinra did not abrogate all evidence of neutrophil activation. There were no statistically significant differences versus control in total number of all leukocytes, neutrophils, or platelets in mice exposed to high pressure (data not shown).

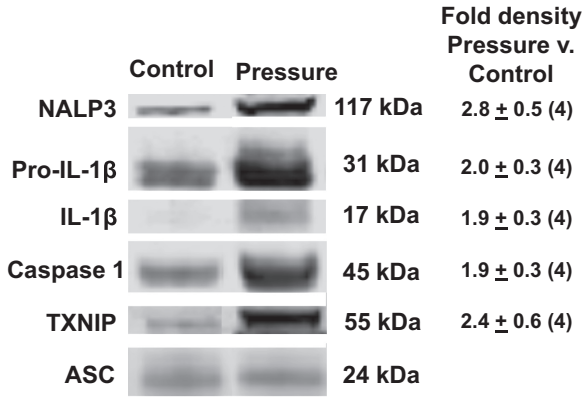

Fig. 4. Protein associations with ASC in neutrophils. Western blots were obtained after neutrophils from control mice and those euthanized 2 h post decompression had been treated with dithiobis (succinimidyl propionate) to cross-link proteins (see MATERIALS AND METHODS). Cell lysates were subjected to immunoprecipitation using antibody to ASC. This is a representative blot among four replicate experiments. After Western blotting, protein band densities were quantified and normalized to the ASC band in each lysate. Ratio of each protein relative to ASC was compared with that calculated for the air-exposed control neutrophils in each experiment. Therefore, data in the figure show the fold-increase in band density normalized to the ratio observed in control cells. Data are mean ± SE ($n = 4$), $P < 0.05$ vs. control in all cases. ASC, apoptosis-associated speck-like protein containing a CARD; IL, interleukin; NALP3, NACHT, LRR, and PYD domains-containing protein 3; TXNIP, thioredoxin-interacting protein.

MPs versus exosomes. MPs and exosomes can carry IL-1β, and we were interested in exploring whether both may be involved with pressure/decompression events (12, 22). The standard 15,000-*g* plasma centrifugation used in preparation for particle analysis does not separate MPs from exosomes. The exosome count in the 15,000-*g* supernatant from control mice was 8.1 ± 1.9 ($n = 7$) × 10^9 particles/ml and from mice euthanized on decompression after 2 h at pressure, 8.5 ± 2.7 [$n = 6$, not statistically significantly different (NS) vs. control] × 10^9 particles/ml. The mean particle diameter for control samples was 89.8 ± 7.6 nm ($n = 7$) and for decompression samples, 90.3 ± 9.1 nm ($n = 6$, NS vs. control).

Whereas exosomes can be sedimented by centrifugation at 100,000 *g* or more, MPs are also in the pellet (12, 22). We found, however, that when 15,000-*g* supernatant samples were centrifuged at 21,000 *g*, the majority of IL-1β in samples was found in pellets: 79.0 ± 6.2% for control and 91.9 ± 2.4% ($n = 6$, NS vs. control) for samples 2 h post decompression, and up to half of the MPs were sedimented [35.0 ± 24% for

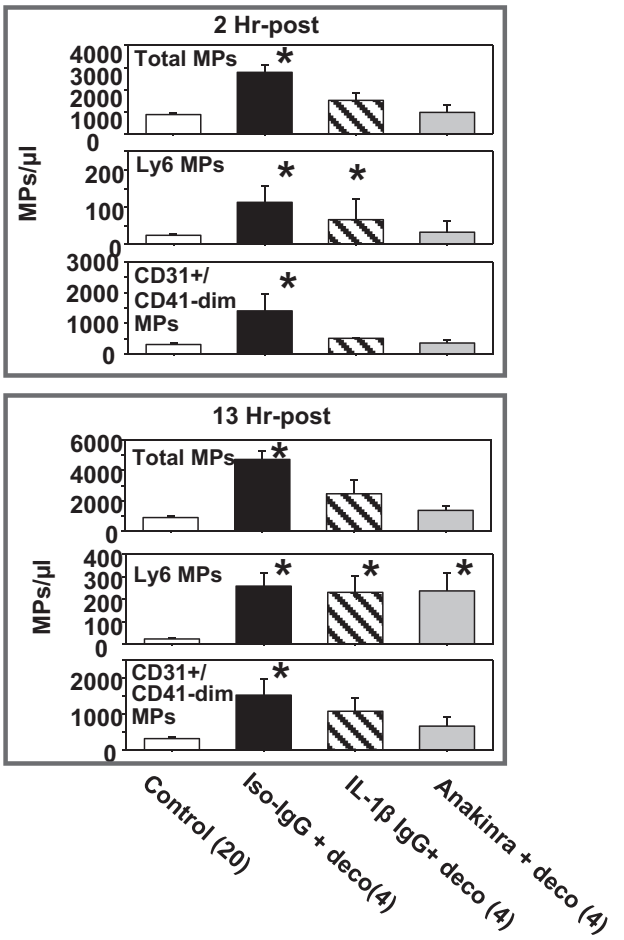

Fig. 5. MPs numbers in mice injected with IL-1β antagonizing agents. Data show blood-borne MPs number in mice injected with either a control IgG, a neutralizing antibody to IL-1β, or anakinra before pressurization and euthanized 2 h or 13 h post decompression. Data are mean ± SE, *n* is as shown, $*P < 0.05$ ANOVA. Deco, decompression; IL, interleukin; Iso IgG, control IgG; MPs, microparticles.

control mice, 51.7 ± 24% ($n = 6$, NS) post decompression]. As expected, exosome counts were not significantly different in 21,000-*g* supernatants: control 9.6 ± 4.6 ($n = 4$) × 10^9 particles/ml and post-decompression 9.7 ± 5.7 ($n = 5$) × 10^9 particles/ml. Western blots performed with particles pelleted by 100,000-*g* centrifugation of samples that had first been subjected to 21,000-*g* centrifugation to remove most IL-1β contained the expected exosome proteins, including prominent bands for lysosome associated membrane protein-1 (LAMP-1) and variable amounts of CD81 and actin, but pro- and mature IL-1β were not detected (data not shown) (64, 69).

IL-1β and other inflammatory mediators. We investigated MPs number and particle cargo from mice injected with anti-IL-1β or anakinra. As shown in Table 2, IL-1β was not statistically significantly elevated in plasma from these mice post decompression, consistent with the autocatalytic actions of IL-1β. Moreover, MPs at both 2 and 13 h post decompression were not elevated over control compared with mice treated with a control, nonspecific IgG (Fig. 5). Next, Western blots of MPs were prepared because we wished to directly compare content of alternative inflammatory mediators. To achieve this, MPs in the standard 15,000-*g* supernatants were counted, and a volume containing exactly 10,000 MPs was centrifuged at 21,000 *g* so that MPs pellets and supernatant from the same samples could be compared. As shown in a representative blot in Fig. 6, pelleted MPs but not the plasma supernatants contained several inflammatory mediators. Band densities were compared against control samples run with each replicate study, and the data demonstrate significantly denser bands in post-decompression samples but not in samples from mice first injected with anakinra before pressure exposure. There were elevations of pro- and mature IL-1β, IL-6, pro- and mature TNF-α, and caspase-1.

We were also interested to see whether components of the NF-κB inflammatory pathway might be involved. NF-κB was not detected in any samples (data not shown), but there were elevations of the inhibitor of κB kinase (IKK)-β and IKK-γ. Moreover, as shown, mice injected with anakinra before pressure exposure did not exhibit these inflammatory protein elevations. Actin band densities are included in the blot merely to demonstrate variability so that it cannot be used as a reliable loading control. We conclude from the work thus far that most blood-borne IL-1β is present within MPs, not exosomes, and so we also expressed plasma IL-1β quantified by ELISA as pg/million MPs in Table 2.

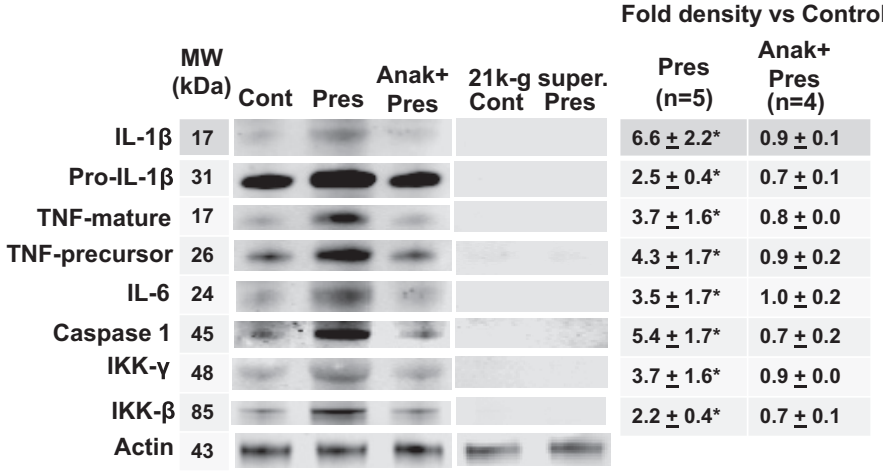

Fig. 6. Representative Western blot of supernatant and pellet fractions. Plasma samples were prepared from control mice (Cont), mice euthanized 2 h after 2 h exposure to 790 kPa (Pres), and mice first injected with anakinra and euthanized 2 h after 2 h exposure to 790 kPa (Anak + Pres). As described in MATERIALS AND METHODS, plasma was initially centrifuged at 15,000 *g* and supernatant containing 10,000 MPs then centrifuged at 21,000 *g*. SDS buffer was added to the MPs pellet and supernatant fractions to maintain exact comparisons, and 20 μg protein was loaded to each lane. Data show mean ± SE fold-elevation in band densities vs. control from replicate studies, *n* is as listed, $*P < 0.05$ by ANOVA. IKK, inhibitor of κB kinase; IL, interleukin; MPs, microparticles; TNF, tumor necrosis factor.

Absence of detectable levels of IL-6 and TNF-α in plasma supernatants (Fig. 6) was surprising, as these proteins are released by conventional protein secretion. Therefore, we questioned whether the proteins may be adsorbed to the surface of MPs. To address this, MPs from control and 2-h post-decompressed mice were harvested, and exactly 10,000 were suspended in PBS buffer and either left intact or subjected to SDS detergent lysis before spotting onto nitrocellulose paper. Representative images and mean ratios for densities of SDS-lysed/intact samples from replicate studies are shown in Fig. 7. Our view was that if a substantial portion of protein was contained within the MPs, the lysed/intact ratio would be significantly greater than 1.0. This was true for all post-decompression samples except when probed for IL-6. Ratios for all other analyses were significantly greater for post-decompression versus control samples.

DISCUSSION

Our results demonstrate that exposure to elevated air pressure triggers production of MPs containing high concentrations of IL-1β in mice. This is consistent with prior work showing that high pressure noble and inert gases such as N_2 cause oxidative stress and that the resulting activation of MPs production and NLRP3 inflammasome pathways overlap (51, 54). Furthermore, we conclude that IL-1β is required for decompression-induced vascular injury manifested as elevations of endothelial MPs (Fig. 1) and diffuse vascular leak based on inhibitory actions of IL-1β neutralizing antibody and receptor antagonist (Fig. 2).

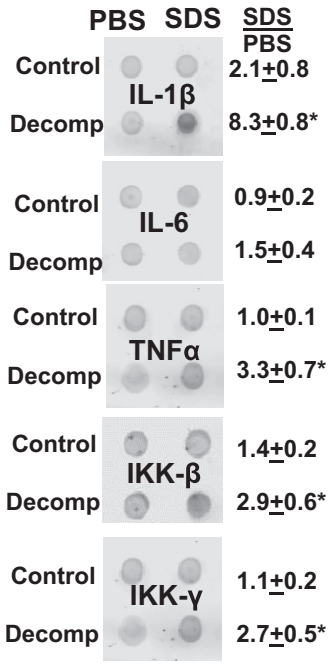

Fig. 7. Dot blot of MPs. Plasma from control mice and mice euthanized at 2 h post decompression (Decomp) were manipulated as described in MATERIALS AND METHODS. Samples containing 10,000 MPs were suspended in PBS or SDS-containing PBS to cause particle lysis and applied to nitrocellulose paper, and blots were subjected to antibody treatments. Numbers reflect the ratio of dot density in the SDS- vs. PBS-suspended MPs. Values are mean ± SE from 6 replicate studies. *Ratio value greater than control ($P < 0.05$, *t*-test). IKK, inhibitor of κB kinase; IL, interleukin; MPs, microparticles; TNF, tumor necrosis factor.

Neutrophils and possibly platelets have been implicated in decompression pathophysiology in previous studies (55, 57, 66). Neutrophils are peculiar among innate immune cells in that they possess some preformed IL-1β, but as with most cells, ongoing production requires protein synthesis that occurs in response to a variety of stimuli (11). The responses in mice euthanized immediately upon decompression from only 1 or 2 h at pressure indicate that pathways for MPs generation (Fig. 1) and NLRP3 inflammasome activation/IL-1β production (Table 2, Figs. 3 and 4) are stimulated while at high gas pressure. The data also indicate that neutrophil-platelet aggregates occur at pressure and are inhibited by anti-IL-1β antibody and anakinra (Table 2). Furthermore, some more traditional parameters of neutrophil activation, such as degranulation with MPO displayed on the membrane surface, occur at pressure and persist, whereas others, such as PR3 and TLR4 expression, develop post decompression (Table 2). Some of these events appear to be independent of IL-1β, as administration of anti-IL-1β or anakinra did not abrogate all indices of neutrophil activation. They may arise because of bubble stimulation or, possibly, high gas pressure mediated oxidative stress.

NLRP3 inflammasome proteins are found in neutrophil cytoplasm, but their co-localization to various cell structures is thought to differ with time following activation (1a, 43). The differences in appearance of NALP3-ASC co-localizations in neutrophils isolated at *time 0* versus 2 h post decompression (Fig. 3) indicate an evolution of inflammasome responses that will require further investigation. It is surprising that among circulating leukocytes, we did not see activation in the lymphocyte population (Figs. 3 and 4). This may be due to differences in the redox enzyme armamentarium, as prior work has suggested a role for MPO (57). It will be important in future work to assess whether pressure activates other leukocyte populations, such as eosinophils, tissue macrophages, microglia, and/or astrocytes.

There were differences noted in the duration of protective efficacy between anti-IL-1β and anakinra for vascular leak, especially in omentum (Fig. 2, *B* and *C*). Local differences in organ/tissue responses may relate to vasculature or, perhaps in the case of tissues like omentum, peculiarities in local fats/lipids (23, 33). Of course, there can also be differences related to pharmaceutical sites of action. The receptor-blocking action of anakinra exceeds 21 h, despite its short plasma half-life of ~1.8 h (17, 19). IgG plasma half-life in mice is days long, but how the antibody is able to disrupt IL-1β-to-receptor interactions despite cytokine encapsulation within MPs is unclear (24).

Findings regarding elevations of IL-6, TNF-α, caspase-1, IKK-β, and IKK-γ associated with MPs indicate an additional level of complexity to high pressure responses. Elevations of all inflammatory mediators were inhibited in pressure-exposed mice treated with anti-IL-1β and anakinra (Table 2, Fig. 6). We interpret this result as evidence for the central role of IL-1β mediating elevations of the other factors, and there is precedence for primacy of IL-1β in other disorders (11). A similar response has been reported focused on TNF-α, where reductions in EVs number as well particle content of IL-6 and TNF-α were found for microglia in response to lipopolysaccharide, and in vivo mouse responses to cerebral ischemic injury after administration of a TNF-α inhibitor, and in TNF-α knockout mice (68). The inflammatory proteins associated with

MPs could all play roles in vascular leak development as well as other manifestations of post-decompression injuries (57, 58, 66). Further work is needed to determine how the various inflammatory mediators may exacerbate MPs generation and enzyme activity needed for gas nuclei generation leading to overt bubble production (57, 58, 66, 67).

We are especially intrigued by the presence of IKK-β and IKK-γ in MPs, which suggests that aspects of the NF-κB pathway may be involved in high pressure pathophysiology. Their presence in MPs has not been reported previously. Others have shown that MPs can induce NF-κB activation, but direct donation of IKKs was not evaluated (4). The IKK complex, consisting of IKK-α and/or IKK-β catalytic units and IKK-γ, a regulatory scaffold protein, initiates activation by phosphorylating IκB (inhibitor of κBs), which triggers its proteasomal degradation, allowing NF-κB nuclear translocation (49). NF-κB plays a quintessential role in transcriptional regulation of inflammation, and there are also less well recognized nongenomic roles for IKK-β (7, 49).

We need also to mention some technical aspects to our results. Because the current investigation indicated a special role for IL-1β, we sought to separate MPs from smaller exosomes, as both can carry IL-1β (26, 44). The ability to separate MPs highly endowed with IL-1β from exosomes and other MPs not containing the numerous inflammatory mediators by centrifugation at 21,000 *g* is novel (see Fig. 6). Whether this manipulation can be used with particles generated in response to alternative stresses is unknown (26, 27, 44). Additionally, IL-6 was found to be adsorbed to the MPs surface, while TNF-α is contained within MPs (Fig. 7). Both IL-6 and TNF-α are processed by conventional protein secretion but can be associated with exosomes (68) and MPs (50). Particle associations of cytokines obviously presents a potential for additional levels of control over cell targeting, and the results also pose some intriguing questions. IL-6 actions differ from those of TNF-α, and they are delivered to different sites at the plasma membrane before secretion (18, 39, 42, 60).

We did not find a difference in plasma exosome counts between control and decompressed mice. As MPs and exosomes are processed by different pathways, this may not seem surprising, although both particle types are often elevated in response to the same stresses (10, 48). TRPS methodology, as we used to count exosomes, may inflate the count because of inclusion of some large protein aggregates. However, results do not support a pathophysiological role for these small particles in decompression-induced vascular injury based on the absence of IL-1β in the exosome-containing 21,000-*g* plasma supernatant (Fig. 6).

In conclusion, the present study advances our understanding of high gas pressure pathophysiology. Demonstration of in vivo responses during pressure exposure shifts the focus on sites of action for "decompression" sickness and highlights the notion that it is an inflammatory disease. The results do not contradict the extensive work showing involvement of bubbles in DCS (9, 41, 71). Rather, they offer a feasible biochemical and physiological mechanism for bubble nuclei production and, because bubbles and inflammatory stimuli both exacerbate MPs formation, MPs can establish a feed-forward or synergistic pathological process (14, 57, 58, 65–67, 70). A more pragmatic aspect to our results is the evidence that pharmaceuticals can be useful to prevent injuries when provocative exposures are to be undertaken. Overall, the data suggest that temporal events in response to high pressure start with cell activation, then inflammasome plus MPs pathways are activated, but responses then differ when looking at the tissue level (based on differences in protective efficacy of anakinra and anti-IL-1β). The absence of plasma IL-1β elevations in anti-IL-1β and anakinra-treated mice (Table 2) indicate IL-1β synthesis occurs as an auto-activation cascade, as is typically seen with inflammatory responses (11). Moreover, finding that these interventions abrogate elevations of MPs (Fig. 5) supports the overlap in pathways responsible for MPs production and NLRP3 activation (51, 52, 54).

GRANTS

This project was supported by Office of Naval Research Grant N00014–16–1-2868 and an unrestricted grant from the National Foundation of Emergency Medicine.

DISCLOSURES

No conflicts of interest, financial or otherwise, are declared by the authors.

AUTHOR CONTRIBUTIONS

S.R.T. conceived and designed research; S.R.T., V.M.B., K.Y., and M.Y. performed experiments; S.R.T. analyzed data; S.R.T. interpreted results of experiments; S.R.T. prepared figures; S.R.T. drafted manuscript; S.R.T., V.M.B., K.Y., and M.Y. edited and revised manuscript; S.R.T., V.M.B., K.Y., and M.Y. approved final version of manuscript.

REFERENCES

1. **Bădulescu O, Bădescu C, Ciocoiu M, Bădescu M.** Interleukin-1-beta and dyslipidemic syndrome as major risk factors for thrombotic complications in type 2 diabetes mellitus. *Mediators Inflamm* 2013: 1–8, 2013. doi:10.1155/2013/169420.

1a. **Bakele M, Joos M, Burdi S, Allgaier N, Pöschel S, Fehrenbacher B, Schaller M, Marcos V, Kümmerle-Deschner J, Rieber N, Borregaard N, Yazdi A, Hector A, Hartl D.** Localization and functionality of the inflammasome in neutrophils. *J Biol Chem* 289: 5320–5329, 2014. doi:10.1074/jbc.M113.505636.

2. **Bao XC, Chen H, Fang YQ, Yuan HR, You P, Ma J, Wang FF.** Clopidogrel reduces the inflammatory response of lung in a rat model of decompression sickness. *Respir Physiol Neurobiol* 211: 9–16, 2015. doi:10.1016/j.resp.2015.02.003.

3. **Barak OF, Mladinov S, Hoiland RL, Tremblay JC, Thom SR, Yang M, Mijacika T, Dujic Z.** Disturbed blood flow worsens endothelial dysfunction in moderate-severe chronic obstructive pulmonary disease. *Sci Rep* 7: 16929, 2017. doi:10.1038/s41598-017-17249-6.

4. **Bardelli C, Amoruso A, Federici Canova D, Fresu L, Balbo P, Neri T, Celi A, Brunelleschi S.** Autocrine activation of human monocyte/macrophages by monocyte-derived microparticles and modulation by PPARγ ligands. *Br J Pharmacol* 165: 716–728, 2012. doi:10.1111/j.1476-5381.2011.01593.x.

5. **Bianco F, Pravettoni E, Colombo A, Schenk U, Möller T, Matteoli M, Verderio C.** Astrocyte-derived ATP induces vesicle shedding and IL-1 beta release from microglia. *J Immunol* 174: 7268–7277, 2005. doi:10.4049/jimmunol.174.11.7268.

6. **Bigley NJ, Perymon H, Bowman GC, Hull BE, Stills HF Jr, Henderson RA.** Inflammatory cytokines and cell adhesion molecules in a rat model of decompression sickness. *J Interferon Cytokine Res* 28: 55–63, 2008. doi:10.1089/jir.2007.0084.

7. **Chariot A.** The NF-kappaB-independent functions of IKK subunits in immunity and cancer. *Trends Cell Biol* 19: 404–413, 2009. doi:10.1016/j.tcb.2009.05.006.

8. **Chen Y, Montcalm-Smith E, Schlaerth C, Auker C, McCarron RM.** Acclimation to decompression: stress and cytokine gene expression in rat lungs. *J Appl Physiol (1985)* 111: 1007–1013, 2011. doi:10.1152/japplphysiol.01402.2010.

9. **Cialoni D, Pieri M, Balestra C, Marroni A.** Dive risk factors, gas bubble formation, and decompression illness in recreational SCUBA diving:

analysis of DAN Europe DSL data base. *Front Psychol* 8: 1587, 2017. doi:10.3389/fpsyg.2017.01587.
10. **Colombo M, Raposo G, Théry C.** Biogenesis, secretion, and intercellular interactions of exosomes and other extracellular vesicles. *Annu Rev Cell Dev Biol* 30: 255–289, 2014. doi:10.1146/annurev-cellbio-101512-122326.
11. **Dinarello CA.** Immunological and inflammatory functions of the interleukin-1 family. *Annu Rev Immunol* 27: 519–550, 2009. doi:10.1146/annurev.immunol.021908.132612.
12. **Dupont N, Jiang S, Pilli M, Ornatowski W, Bhattacharya D, Deretic V.** Autophagy-based unconventional secretory pathway for extracellular delivery of IL-1β. *EMBO J* 30: 4701–4711, 2011. doi:10.1038/emboj.2011.398.
13. **Eftedal OS, Lydersen S, Brubakk AO.** The relationship between venous gas bubbles and adverse effects of decompression after air dives. *Undersea Hyperb Med* 34: 99–105, 2007.
14. **Eppensteiner J, Davis RP, Barbas AS, Kwun J, Lee J.** Immunothrombotic activity of damage-associated molecular patterns and extracellular vesicles in secondary organ failure induced by trauma and sterile insults. *Front Immunol* 9: 190, 2018. doi:10.3389/fimmu.2018.00190.
15. **Ersson A, Linder C, Ohlsson K, Ekholm A.** Cytokine response after acute hyperbaric exposure in the rat. *Undersea Hyperb Med* 25: 217–221, 1998.
16. **Ersson A, Walles M, Ohlsson K, Ekholm A.** Chronic hyperbaric exposure activates proinflammatory mediators in humans. *J Appl Physiol (1985)* 92: 2375–2380, 2002. doi:10.1152/japplphysiol.00705.2001.
17. **Fox E, Jayaprakash N, Pham TH, Rowley A, McCully CL, Pucino F, Goldbach-Mansky R.** The serum and cerebrospinal fluid pharmacokinetics of anakinra after intravenous administration to non-human primates. *J Neuroimmunol* 223: 138–140, 2010. doi:10.1016/j.jneuroim.2010.03.022.
18. **Ghoreschi K, Laurence A, Yang XP, Tato CM, McGeachy MJ, Konkel JE, Ramos HL, Wei L, Davidson TS, Bouladoux N, Grainger JR, Chen Q, Kanno Y, Watford WT, Sun HW, Eberl G, Shevach EM, Belkaid Y, Cua DJ, Chen W, O'Shea JJ.** Generation of pathogenic T(H)17 cells in the absence of TGF-β signalling. *Nature* 467: 967–971, 2010. doi:10.1038/nature09447.
19. **Granowitz EV, Porat R, Mier JW, Pribble JP, Stiles DM, Bloedow DC, Catalano MA, Wolff SM, Dinarello CA.** Pharmacokinetics, safety and immunomodulatory effects of human recombinant interleukin-1 receptor antagonist in healthy humans. *Cytokine* 4: 353–360, 1992. doi:10.1016/1043-4666(92)90078-6.
20. **Gurung P, Anand PK, Malireddi RK, Vande Walle L, Van Opdenbosch N, Dillon CP, Weinlich R, Green DR, Lamkanfi M, Kanneganti TD.** FADD and caspase-8 mediate priming and activation of the canonical and noncanonical Nlrp3 inflammasomes. *J Immunol* 192: 1835–1846, 2014. doi:10.4049/jimmunol.1302839.
21. **Han CH, Zhang PX, Xu WG, Li RP, Xu JJ, Liu WW.** Polarization of macrophages in the blood after decompression in mice. *Med Gas Res* 7: 236–240, 2018. doi:10.4103/2045-9912.215749.
22. **Jiang S, Dupont N, Castillo EF, Deretic V.** Secretory versus degradative autophagy: unconventional secretion of inflammatory mediators. *J Innate Immun* 5: 471–479, 2013. doi:10.1159/000346707.
23. **Kaczerska D, Siermontowski P, Olszański R, Krefft K, Małgorzewicz S, Van Damme-Ostapowicz K.** The influence of high-fat diets on the occurrence of decompression stress after air dives. *Undersea Hyperb Med* 40: 487–497, 2013.
24. **Kontermann RE.** Strategies to extend plasma half-lives of recombinant antibodies. *BioDrugs* 23: 93–109, 2009. doi:10.2165/00063030-200923020-00003.
25. **Lachmann HJ, Lowe P, Felix SD, Rordorf C, Leslie K, Madhoo S, Wittkowski H, Bek S, Hartmann N, Bosset S, Hawkins PN, Jung T.** In vivo regulation of interleukin 1beta in patients with cryopyrin-associated periodic syndromes. *J Exp Med* 206: 1029–1036, 2009. doi:10.1084/jem.20082481.
26. **Lacroix R, Plawinski L, Robert S, Doeuvre L, Sabatier F, Martinez de Lizarrondo S, Mezzapesa A, Anfosso F, Leroyer AS, Poullin P, Jourde N, Njock MS, Boulanger CM, Anglés-Cano E, Dignat-George F.** Leukocyte- and endothelial-derived microparticles: a circulating source for fibrinolysis. *Haematologica* 97: 1864–1872, 2012. doi:10.3324/haematol.2012.066167.
27. **Lacroix R, Robert S, Poncelet P, Dignat-George F.** Overcoming limitations of microparticle measurement by flow cytometry. *Semin Thromb Hemost* 36: 807–818, 2010. doi:10.1055/s-0030-1267034.
28. **Lee HC, Chen YS, Kang BH, Wan FJ, Chang LP, Huang KL.** Serum heat shock protein after simulated deep diving in Navy divers. *Chin J Physiol* 52: 295–298, 2009. doi:10.4077/CJP.2009.AMH042.
29. **Little T, Butler BD.** Pharmacological intervention to the inflammatory response from decompression sickness in rats. *Aviat Space Environ Med* 79: 87–93, 2008. doi:10.3357/ASEM.2118.2008.
30. **Liu X, Cao Y, Gao G, Mao R, Bi L, Geng M.** Gene expression profile of type II spinal cord decompression sickness. *Spinal Cord* 52: 606–610, 2014. doi:10.1038/sc.2014.65.
31. **Ljubkovic M, Dujic Z, Møllerløkken A, Bakovic D, Obad A, Breskovic T, Brubakk AO.** Venous and arterial bubbles at rest after no-decompression air dives. *Med Sci Sports Exerc* 43: 990–995, 2011. doi:10.1249/MSS.0b013e31820618d3.
32. **Ljubkovic M, Marinovic J, Obad A, Breskovic T, Gaustad SE, Dujic Z.** High incidence of venous and arterial gas emboli at rest after trimix diving without protocol violations. *J Appl Physiol (1985)* 109: 1670–1674, 2010. doi:10.1152/japplphysiol.01369.2009.
33. **Lonati GL, Westgate AJ, Pabst DA, Koopman HN.** Nitrogen solubility in odontocete blubber and mandibular fats in relation to lipid composition. *J Exp Biol* 218: 2620–2630, 2015. doi:10.1242/jeb.122606.
35. **MacKenzie A, Wilson HL, Kiss-Toth E, Dower SK, North RA, Surprenant A.** Rapid secretion of interleukin-1beta by microvesicle shedding. *Immunity* 15: 825–835, 2001. doi:10.1016/S1074-7613(01)00229-1.
36. **Madden D, Thom SR, Milovanova TN, Yang M, Bhopale VM, Ljubkovic M, Dujic Z.** Exercise before scuba diving ameliorates decompression-induced neutrophil activation. *Med Sci Sports Exerc* 46: 1928–1935, 2014. doi:10.1249/MSS.0000000000000319.
37. **Madden D, Thom SR, Yang M, Bhopale VM, Ljubkovic M, Dujic Z,.** High intensity cycling before SCUBA diving reduces post-decompression microparticle production and neutrophil activation. *Eur J Appl Physiol* 114: 1955–1961, 2014. doi:10.1007/s00421-014-2925-7.
38. **Madden LA, Chrismas BC, Mellor D, Vince RV, Midgley AW, McNaughton LR, Atkin SL, Laden G.** Endothelial function and stress response after simulated dives to 18 msw breathing air or oxygen. *Aviat Space Environ Med* 81: 41–45, 2010. doi:10.3357/ASEM.2610.2010.
39. **Manderson AP, Kay JG, Hammond LA, Brown DL, Stow JL.** Subcompartments of the macrophage recycling endosome direct the differential secretion of IL-6 and TNFalpha. *J Cell Biol* 178: 57–69, 2007. doi:10.1083/jcb.200612131.
40. **Montcalm-Smith E, Caviness J, Chen Y, McCarron RM.** Stress biomarkers in a rat model of decompression sickness. *Aviat Space Environ Med* 78: 87–93, 2007.
41. **Murphy FG, Hada EA, Doolette DJ, Howle LE.** Probabilistic pharmacokinetic models of decompression sickness in humans: Part 2, coupled perfusion-diffusion models. *Comput Biol Med* 92: 90–97, 2018. doi:10.1016/j.compbiomed.2017.11.011.
42. **Murray RZ, Kay JG, Sangermani DG, Stow JL.** A role for the phagosome in cytokine secretion. *Science* 310: 1492–1495, 2005. doi:10.1126/science.1120225.
43. **Naegelen I, Beaume N, Plançon S, Schenten V, Tschirhart EJ, Bréchard S.** Regulation of neutrophil degranulation and cytokine secretion: a novel model approach based on linear fitting. *J Immunol Res* 2015: 1–15, 2015. doi:10.1155/2015/817038.
44. **Orozco AF, Lewis DE.** Flow cytometric analysis of circulating microparticles in plasma. *Cytometry A* 77A: 502–514, 2010. doi:10.1002/cyto.a.20886.
45. **Pizzirani C, Ferrari D, Chiozzi P, Adinolfi E, Sandonà D, Savaglio E, Di Virgilio F.** Stimulation of P2 receptors causes release of IL-1beta-loaded microvesicles from human dendritic cells. *Blood* 109: 3856–3864, 2007. doi:10.1182/blood-2005-06-031377.
46. **Pontier JM, Gempp E, Ignatescu M.** Blood platelet-derived microparticles release and bubble formation after an open-sea air dive. *Appl Physiol Nutr Metab* 37: 888–892, 2012. doi:10.1139/h2012-067.
47. **Qing L, Yi HJ, Wang YW, Zhou Q, Ariyadewa DK, Xu WG.** Hyperbaric oxygen pretreatment benefits on decompression sickness in Bama pigs. *J Exp Biol* 221: jeb171066, 2018. doi:10.1242/jeb.171066.
48. **Redman CW, Tannetta DS, Dragovic RA, Gardiner C, Southcombe JH, Collett GP, Sargent IL.** Review: does size matter? Placental debris and the pathophysiology of pre-eclampsia. *Placenta* 33, *Suppl*: S48–S54, 2012. doi:10.1016/j.placenta.2011.12.006.
49. **Scheidereit C.** IkappaB kinase complexes: gateways to NF-kappaB activation and transcription. *Oncogene* 25: 6685–6705, 2006. doi:10.1038/sj.onc.1209934.

50. **Soni S, Wilson MR, O'Dea KP, Yoshida M, Katbeh U, Woods SJ, Takata M.** Alveolar macrophage-derived microvesicles mediate acute lung injury. *Thorax* 71: 1020–1029, 2016. doi:10.1136/thoraxjnl-2015-208032.
51. **Thom SR, Bhopale VM, Hu J, Yang M.** Increased carbon dioxide levels stimulate neutrophils to produce microparticles and activate the nucleotide-binding domain-like receptor 3 inflammasome. *Free Radic Biol Med* 106: 406–416, 2017. doi:10.1016/j.freeradbiomed.2017.03.005.
52. **Thom SR, Bhopale VM, Hu J, Yang M.** Inflammatory responses to acute elevations of carbon dioxide in mice. *J Appl Physiol (1985)* 123: 297–302, 2017. doi:10.1152/japplphysiol.00343.2017.
53. **Thom SR, Bhopale VM, Mancini DJ, Milovanova TN.** Actin S-nitrosylation inhibits neutrophil beta2 integrin function. *J Biol Chem* 283: 10822–10834, 2008. doi:10.1074/jbc.M709200200.
54. **Thom SR, Bhopale VM, Yu K, Huang W, Kane MA, Margolis DJ.** Neutrophil microparticle production and inflammasome activation by hyperglycemia due to cytoskeletal instability. *J Biol Chem* 292: 18312–18324, 2017. doi:10.1074/jbc.M117.802629.
55. **Thom SR, Milovanova TN, Bogush M, Bhopale VM, Yang M, Bushmann K, Pollock NW, Ljubkovic M, Denoble P, Dujic Z.** Microparticle production, neutrophil activation, and intravascular bubbles following open-water SCUBA diving. *J Appl Physiol (1985)* 112: 1268–1278, 2012. doi:10.1152/japplphysiol.01305.2011.
56. **Thom SR, Milovanova TN, Bogush M, Yang M, Bhopale VM, Pollock NW, Ljubkovic M, Denoble P, Madden D, Lozo M, Dujic Z.** Bubbles, microparticles, and neutrophil activation: changes with exercise level and breathing gas during open-water SCUBA diving. *J Appl Physiol (1985)* 114: 1396–1405, 2013. doi:10.1152/japplphysiol.00106.2013.
57. **Thom SR, Yang M, Bhopale VM, Huang S, Milovanova TN.** Microparticles initiate decompression-induced neutrophil activation and subsequent vascular injuries. *J Appl Physiol (1985)* 110: 340–351, 2011. doi:10.1152/japplphysiol.00811.2010.
58. **Thom SR, Yang M, Bhopale VM, Milovanova TN, Bogush M, Buerk DG.** Intramicroparticle nitrogen dioxide is a bubble nucleation site leading to decompression-induced neutrophil activation and vascular injury. *J Appl Physiol (1985)* 114: 550–558, 2013. doi:10.1152/japplphysiol.01386.2012.
59. **Tremblay JC, Thom SR, Yang M, Ainslie PN.** Oscillatory shear stress, flow-mediated dilatation, and circulating microparticles at sea level and high altitude. *Atherosclerosis* 256: 115–122, 2017. doi:10.1016/j.atherosclerosis.2016.12.004.
60. **Veldhoen M, Hocking RJ, Atkins CJ, Locksley RM, Stockinger B.** TGFbeta in the context of an inflammatory cytokine milieu supports de novo differentiation of IL-17-producing T cells. *Immunity* 24: 179–189, 2006. doi:10.1016/j.immuni.2006.01.001.
61. **Vince RV, McNaughton LR, Taylor L, Midgley AW, Laden G, Madden LA.** Release of VCAM-1 associated endothelial microparticles following simulated SCUBA dives. *Eur J Appl Physiol* 105: 507–513, 2009. doi:10.1007/s00421-008-0927-z.
62. **Wang HT, Fang YQ, Bao XC, Yuan HR, Ma J, Wang FF, Zhang S, Li KC.** Expression changes of TNF-α, IL-1β and IL-6 in the rat lung of decompression sickness induced by fast buoyancy ascent escape. *Undersea Hyperb Med* 42: 23–31, 2015.
63. **Wang HT, Fang YQ, You P, Bao XC, Yuan HR, Ma J, Wang FF, Li KC.** Expression changes of inflammatory factors in the rat lung of decompression sickness induced by fast buoyancy ascent escape. *Undersea Hyperb Med* 42: 15–22, 2015.
64. **Wang J, Yao Y, Wu J, Li G.** Identification and analysis of exosomes secreted from macrophages extracted by different methods. *Int J Clin Exp Pathol* 8: 6135–6142, 2015.
65. **Yu X, Xu J, Huang G, Zhang K, Qing L, Liu W, Xu W.** Bubble-induced endothelial microparticles promote endothelial dysfunction. *PLoS One* 12: e0168881, 2017. doi:10.1371/journal.pone.0168881.
66. **Yang M, Kosterin P, Salzberg BM, Milovanova TN, Bhopale VM, Thom SR.** Microparticles generated by decompression stress cause central nervous system injury manifested as neurohypophysial terminal action potential broadening. *J Appl Physiol (1985)* 115: 1481–1486, 2013. doi:10.1152/japplphysiol.00745.2013.
67. **Yang M, Milovanova TN, Bogush M, Uzun G, Bhopale VM, Thom SR.** Microparticle enlargement and altered surface proteins after air decompression are associated with inflammatory vascular injuries. *J Appl Physiol (1985)* 112: 204–211, 2012. doi:10.1152/japplphysiol.00953.2011.
68. **Yang Y, Boza-Serrano A, Dunning CJR, Clausen BH, Lambertsen KL, Deierborg T.** Inflammation leads to distinct populations of extracellular vesicles from microglia. *J Neuroinflammation* 15: 168, 2018. doi:10.1186/s12974-018-1204-7.
69. **Yoshioka Y, Konishi Y, Kosaka N, Katsuda T, Kato T, Ochiya T.** Comparative marker analysis of extracellular vesicles in different human cancer types. *J Extracell Vesicles* 2: 20424, 2013. doi:10.3402/jev.v2i0.20424.
70. **Yu X, Xu J, Liu W, Xu W.** Bubbles induce endothelial microparticle formation via a calcium-dependent pathway involving flippase inactivation and Rho kinase activation. *Cell Physiol Biochem* 46: 965–974, 2018. doi:10.1159/000488825.
71. **Zhang K, Wang D, Jiang Z, Ning X, Buzzacott P, Xu W.** Endothelial dysfunction correlates with decompression bubbles in rats. *Sci Rep* 6: 33390, 2016. doi:10.1038/srep33390.